Macromolecules

pubs.acs.org/Macromolecules Article

Preparation of Polyphosphorodiamidates by Michael Addition

Nantawat Kaekratoke and Daniel Crespy*

Cite This: Macromolecules 2024, 57, 9396−9407 Read Online

ACCESS | Metrics & More | Article Recommendations | Supporting Information

ABSTRACT: Phosphorus-containing polymers find applications as fire retardant additives and biomimicking macromolecules. Herein, a series of polymers are synthesized by thiol-ene polymerization using a novel, high phosphorus content diacrylate monomer (PNDA) and various aliphatic and aromatic dithiols and amines. Depending on the chemical structure of the dithiol, low molecular weight polymers with relatively low or high glass transition temperatures are obtained. Molecular weight can be increased by copolymerizing the dithiols with PNDA in the presence of other more reactive diacrylates or by polymerizing PNDA with amines. Furthermore, polyhydroxyurethanes were synthesized by derivatizing unsaturated phosphoramidates to epoxides and subsequently to cyclic carbonates, which were then reacted with diamines. We also explore the thermal stability of the polymers as well as their application as a fire retardant additive for epoxy resins.

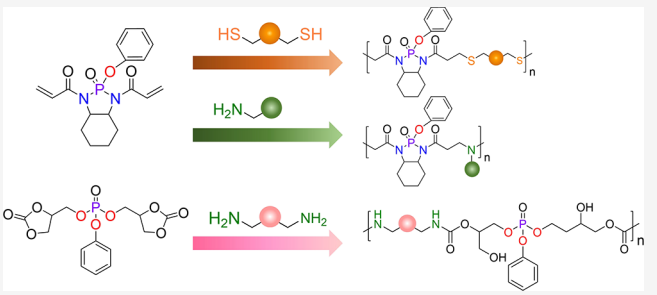

1. INTRODUCTION

In recent decades, polymers with phosphorus in their main chain have attracted significant interest due to their unique properties. These polymers offer a halogen-free approach to materials for flame retardancy,[1] can exhibit proton conductivity,[2] and find applications as binders in dental and bone cements.[3] Their low toxicity and biocompatibility have further fueled research efforts, exploring their potential in biomedical fields.[2,4,5] This includes applications in antifouling coatings,[6,7] antiscalant,[8] tissue engineering,[9] and drug delivery systems.[10] Polymers with phosphorus in their main chain include poly(phosphine oxide)s,[5] poly(phosphonate)s,[11,12] poly(phosphate)s,[13,14] polyphosphazenes,[15,16] polyphosphoramidates,[14,17] polyphosphonamides,[18] polyphosphorodiamides,[19] and polyphosphoramides.[20]

Poly(phosphine oxide)s hold promise as a material to fabricate proton exchange membranes due to their excellent proton conductivity.[21] Phosphonium-based polymers and ionic liquids are promising candidates for the next-generation battery electrolytes due to their inherent ionic conductivity and thermodynamic stability. Combining ionic liquids with lithium salts enhanced electrochemical stability, reduced electrolyte decomposition, and extended battery cycle life. Additionally, the nonflammability and low volatility of ionic liquids improved safety and high-temperature performance.[22,23] Phosphorus-based polymers like polyphosphates, polyphosphonates, and polyphosphoesters are gaining traction in biomedicine due to their biodegradability,[24] blood compatibility,[25] reduced protein adsorption, and strong interactions with hard tissues.[2] Organophosphonates and poly(phosphonate)s exhibit interesting complex properties, allowing them to form strong bonds with metal ions.[8,26,27] Phosphorus-containing flame retardant polymers were suggested as a safer alternative to traditional halogenated options. They form a protective layer that extinguishes fires by limiting oxygen supply, while also preventing the release of toxic gases and bioaccumulation.[28−31] A synergistic effect for flame retardancy between phosphorus (P) and nitrogen (N) atoms was demonstrated, significantly enhancing the effectiveness of phosphorus-based flame retardants.[32,33,30,34] Phosphorus combined with another element can enhance flame retardancy through a synergistic effect. Nitrogen-containing flame retardants effectively reduce smoke and toxic gas emissions during combustion. The nonflammable gases (N_2, NH_3) released during combustion dilute oxygen near the burning surface, enhancing flame retardancy.[1,28,35] Phosphorus-containing flame retardants primarily differ in their gas and condensed-phase activity. In the condensed phase, phosphorus-containing materials promote char formation, trapping fuel and acting as a heat shield.[1,28,35] This occurs through dehydration, phosphoric acid formation, cross-linking, and aromatization.[1,28,35] In the gas phase, PO radicals inhibit combustion by slowing down exothermic radical reactions, reducing heat release.[1,28,35] Polymers with phosphorus-nitrogen bonds include polyphosphazenes,[15,16] polyphosphorami-

Received: June 6, 2024
Revised: September 3, 2024
Accepted: September 17, 2024
Published: September 24, 2024

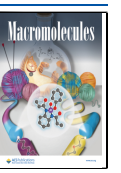

https://doi.org/10.1021/acs.macromol.4c01288
Macromolecules 2024, 57, 9396−9407

Scheme 1. Comparison between Previous Strategies and Current Work for Synthesizing Polyphosphorodiamidates (PPDAs)[a]

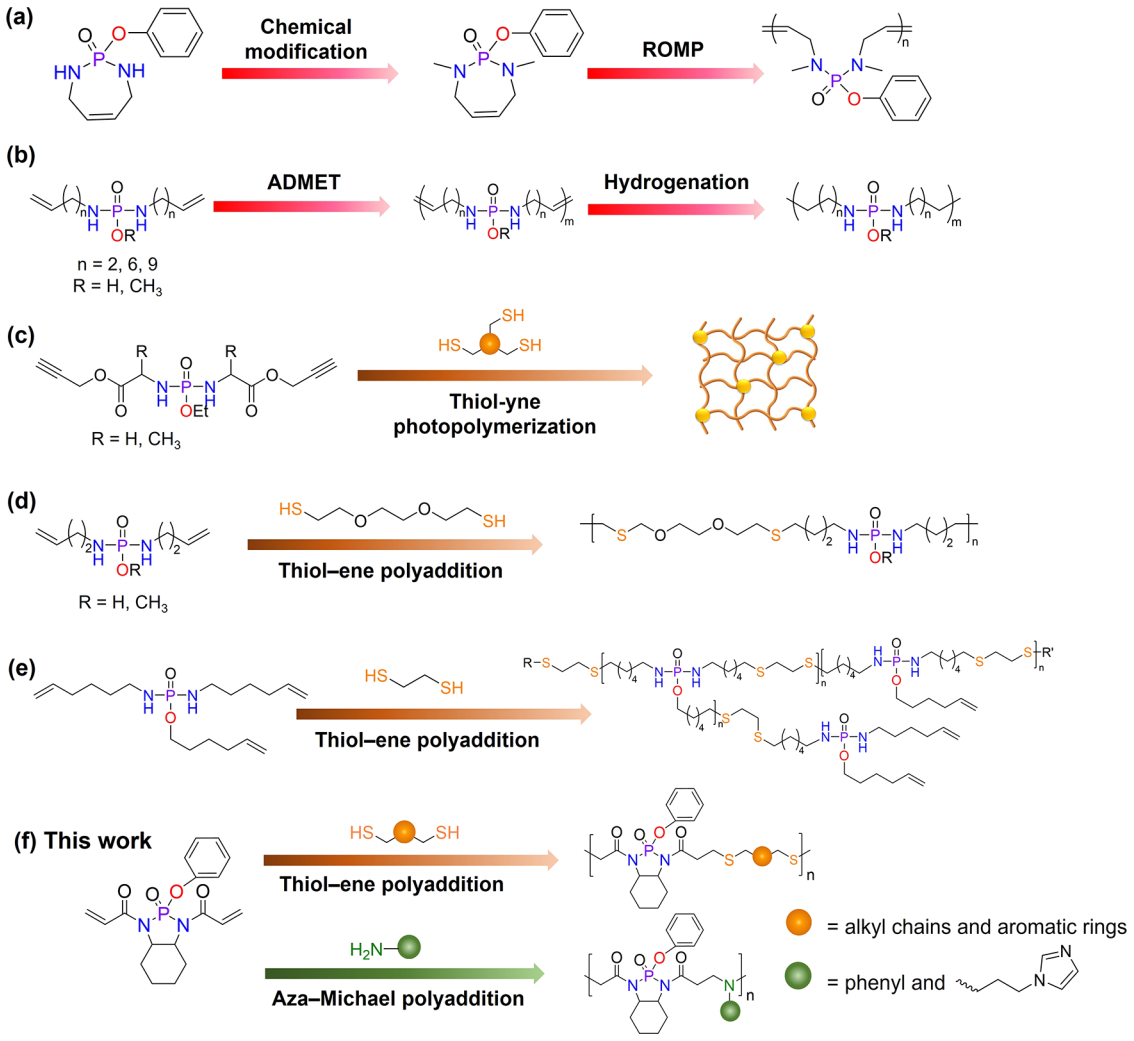

[a]Polymers were synthesized by (a) ring-opening metathesis polymerization (ROMP), (b) acyclic diene metathesis (ADMET) polymerization, (c) thiol-yne photopolymerization,[41] (d–f) thiol-ene and (f) aza-Michael polyaddition.

dates,[14,17] polyphosphonamides,[18] polyphosphorodiamides,[19] and polyphosphoramides.[20] Polyphosphorodiamidates (PPDAs) contain phosphorodiamidate groups (−P(O)−(OR)(NHR)$_2$) in their backbone, where R can be a hydrogen or any organic substituent. Polymers with phosphorodiamidate linkages in their main chain have only been scarcely studied, with most reports on inflammation-targeted delivery,[36−38] as antisense or anticancer therapeutics,[39,40] gene delivery,[41] or aromatic flame retardants (see Scheme 1).[28,42]

Phosphorodiamidate monomers containing either P-OH or P-OCH$_3$ side groups were subjected to acyclic diene metathesis (ADMET) polycondensation to form oligomers (Scheme 1), which displayed superior thermal stability compared to analogous polyphosphoesters.[19] A phosphoramidate containing cyclic olefin, 1,3-dimethyl-2-phenoxy-1,3,4,7-tetrahydro-1,3,2-diazaphosphepine-2-oxide could be polymerized at room temperature with 84% conversion within 30 min, leading to relatively high molecular weight (up to 80 kDa).[36−38] The major limitation of these metathesis reactions is however the need of expensive metal catalysts and the necessary post-polymerization hydrogenation to obtain polymers with saturated bonds.

To overcome this issue, an alternative is the preparation of PPDAs by metal-free thiol-ene polymerization.[28,43] Thiol-ene polyaddition is attractive due to its tolerance for diverse functional groups and its ability to achieve high conversion rates. Water-soluble PPDAs prepared by thiol-ene polymerization (Scheme 1) rapidly degraded under acidic conditions due to hydrolysis of the main chain, while the P−N bonds remain relatively stable under basic conditions.[43] Cross-linked resins with tunable degradation and low cytotoxicity were prepared by the polymerization of polyphosphorodiamidate monomers bearing alkyne groups based on amino acid structures and hydrophobic thiols under UV light.[44] Phosphorodiamidate monomers as B$_3$-monomers and 1,2-ethanedithiol as A$_2$-comonomers were reacted to undergo thiol-ene polyaddition to form the hyperbranched polymers (Scheme 1).[28] The polymers were used as flame retardant additives in epoxy resins. The hyperbranched PPDAs exhibited both a higher glass transition temperature and a larger residue yield after pyrolysis compared to hyperbranched polyphosphates.[28] However, the reported PPDAs displayed relatively low glass transition temperatures (−62 to 42 °C).[19,28,37]

To address these limitations and explore the influence of a monomer structure on thermal stability, we designed and

https://doi.org/10.1021/acs.macromol.4c01288
Macromolecules 2024, 57, 9396−9407

synthesized a new series of PPDAs that can promote stronger intermolecular interactions using efficient thiol-ene click chemistry with various commercially available aliphatic and aromatic dithiols and amines. These novel PPDAs were comprehensively characterized applied as flame retardant opens in epoxy resins.

2. EXPERIMENTAL SECTION

2.1. Materials. Phenyl phosphorodichloridate (>98%, TCI), *trans*-1,2-diaminocyclohexane (>97%, TCI), triethylamine (Et_3N, > 99%, Carlo Erba), 1,2-ethanedithiol (EDT, > 95%, Acros), 2,2′-(ethylenedioxy) diethanethiol (EDDT, >95%, Acros), 4-(4-sulfanylphenyl)-sulfanylbenzenethiol (4,4′-TBBT, >98%, Acros), 6-(dibutylamino)-1,3,5-triazine-2,4-dithiol (TADT, >98%, TCI), 2,5-dimercapto-1,3,4-thiadiazole (DMTD, >95%, TCI), aniline (99%, Panreac), 1-(3-aminopropyl)imidazole (Apim, 97%, TCI), hydroquinone (99%, TCI), glycerol 1,2-carbonate (>90%, TCI), 1,6-diaminohexane (HMDA, 99%, TCI,) *m*-xylylenediamine (*m*−XDA, 99%, TCI), dimethylformamide (DMF, > 99%, Acros), dimethyl sulfoxide (DMSO, 99.9%, Acros), 1,1′-azobis(cyclohexanecarbonitrile) (ABCN, > 98%, Sigma), 2,2-bis(hydroxymethyl)propionic acid (DMPA, 98%, Acros), diglycidyl ether of bisphenol A (DGEBA, TCI, >85%), 2,2′-dimethyl-4,4'-methylene-bis(cyclohexylamine) (DMC, TCI, 99%), anhydrous dichloromethane stabilized with 2-methyl-2-butene (>99%, TCI), DMSO-d_6 (>99.9% atom D, Merck), $CDCl_3$ (>99.9% atom D, Merck), dichloromethane (DCM, 99%, Italmar), methanol (99.9%, Italmar), ethyl acetate (99.9%, Italmar), anhydrous sodium sulfate (>99%, Italmar), sodium chloride (>99%, Italmar), and precoated silica gel (60F254, Merck) were used without further purification. Acryloyl chloride was synthesized following a previous report.[45]

2.2. Analytical Tools. ^1H, ^{13}C, and ^{31}P NMR spectra were recorded on a Bruker 600 MHz NMR spectrometer at room temperature in DMSO-d_6. To determine the molecular weight of the polymers by 2D DOSY (diffusion ordered spectroscopy) NMR, PMMA with known molecular weights and molar weight distribution were dissolved in DMSO-d_6 (~1.0 mg mL^{-1}). The duration of the gradient pulse (δ) was set to 1400 μs and the diffusion time (Δ) to 0.06 s. All experiments were run without spinning to minimize convection, and a maximum gradient strength was 50 G cm^{-1} and 32 linear gradient steps. The data were recorded automatically by the ICON−NMR software (Bruker Biospin, Rheinstetten, Germany). All NMR spectra were manually phased and baseline-corrected using TopSpin 4.1.4 (Bruker Biospin, Rheinstetten, Germany). The PMMA standards have been used because of their availability. We selected PMMA because it is less hydrophobic than polystyrene and less hydrophilic than poly(ethylene oxide). Although the chemical structures of the polyphosphorodiamidates are not similar to PMMA, we believe that they are also less hydrophobic than polystyrene and more hydrophobic than poly(ethylene oxide). Thermal properties were measured by thermal gravimetry analysis (TGA, TGA-DTA8122, Rigaku) from 40 to 700 °C at a rate of 10 °C min^{-1} under a nitrogen atmosphere of 100 SCCM·min^{-1}. Glass transition temperatures (T_g) were determined by differential scanning calorimetry (DSC, DSC 8500, PerkinElmer) with three heating and cooling runs were performed at a rate of 10 K min^{-1} with a flow rate of 50 mL min^{-1} under nitrogen atmosphere between −40 and 180 °C. The T_g of polymers and flame retardant epoxy resins were an average of values obtained from the second and third heating runs. The molecular weights of the polymers were determined by gel permeation chromatography (GPC, model Viscotek TDAmax, Malvern). The polymers were dissolved in THF with a concentration of 3 mg mL^{-1}, and the polymer solutions were filtrated through a PTFE membrane filter (0.22 mm pore size). Three single-pore GPC/SEC columns (6, 7, and 10 μm particle size, linear M) were heated at 35 °C, while a flow rate of 1 mL min^{-1} and a RI-detector were used. Polystyrenes from PSS (Mainz) with different molecular weights and narrow molar weight dispersion were used for calibration. X−ray photoelectron spectroscopy (XPS) was performed with a JPS-9010MC apparatus from JEOL with a Mg K_α source (1253.6 eV) at 250 W. All samples were measured under high vacuum pressure in the range 10^{-8} Pa at room temperature. The molar mass of PN and PNDA was determined by liquid chromatography quadrupole time-of-flight mass spectrometry (LC-Q-TOF-MS, model Compact QTOF, Bruker). Limiting oxygen index (LOI, No.214, Yasuda, Japan) measurements were performed in accordance with ASTM D2863. The flame−retardant epoxy samples corresponded to type IV of the standard (dimensions: 130 mm × 6.5 mm × 3 mm). All samples were stored at 23 °C and 50% relative humidity for at least 80 h before measurements. Underwriter's Laboratory 94 (UL-94, LR-K001, Lonroy, China) measurements were performed on samples (125 mm × 13 mm × 3 mm) stored at 23 °C and 50% relative humidity for at least 80 h in vertical and horizontal orientations according to EN 60695-11-10.

2.3. Synthesis of 2-Phenoxyoctahydrobenzo[*d*][1,3,2]-diazaphosphole 2-oxide (PN). Diphenyl phosphorochloridate (500 mg, 2.37 mmol, 354 μL) was dissolved in dry dichloromethane (10 mL), and the solution was cooled to 0 °C in an ice bath. A solution of *trans*-1,2-diaminocyclohexane (595 mg, 5.21 mmol, 626 μL) and triethylamine (599 mg, 5.93 mmol, 826 μL) in dry dichloromethane (10 mL) was added dropwise over 30 min at 0 °C. The mixture was then allowed to gradually warm up to 25−30 °C and stirred for an additional 12 h. Then, the mixture was extracted with water, and the organic layer was collected and dried over Na_2SO_4. The solvent was removed under reduced pressure, and the crude product was purified by column chromatography. Elution was conducted with a mixture of dichloromethane and methanol. The solvent was removed with a rotary evaporator to obtain PN as a yellow powder with a yield of 83%. ^1H NMR spectroscopy, (600 MHz, DMSO-d_6), δ (ppm): 7.34−7.32 (t, 2H), 7.17−7.15 (d, 1H), 7.14−7.11 (m, 2H), 5.26−5.25 (d, 1H), 5.06−5.05 (d, 1H), 2.86−2.83 (t, 1H), 2.47−2.45 (t, 1H), 1.74−1.71 (m, 2H), 1.60−1.56 (m, 2H), 0.97−1.27 (m, 4H) (Figure S1). ^{13}C NMR spectroscopy, (600 MHz, DMSO-d_6), δ (ppm): 151.8, 129.2, 123.8, 121.0, 60.2, 59.6, 30.9, 30.3, 23.8 (Figure S2). ^{31}P NMR spectroscopy, (600 MHz, DMSO-d_6), δ (ppm): 26.0 (s) (Figure S3). Calcd for $C_{12}H_{17}N_2O_2P$ 253.1100 $[M + H]^+$, found 253.1485.

2.4. Synthesis of 1,1′-(2-Oxido-2-phenoxyhexahydrobenzo-[*d*][1,3,2]diazaphosphole-1,3-diyl)bis(prop-2-en-1-one) (PNDA). PN (500 mg, 1.98 mmol) and triethylamine (501 mg, 4.95 mmol, 691 μL) were dissolved in dry dichloromethane (10 mL), and the solution was cooled to 0 °C in an ice bath. A solution of acryloyl chloride (394 mg, 4.36 mmol, 352 μL) in dry dichloromethane (10 mL) was added dropwise over 30 min at 0 °C. The mixture was then allowed to gradually warm up to 25−30 °C and stirred for an additional 12 h. Then, the mixture was extracted three times with water, and the organic layer was collected and dried over Na_2SO_4. The solvent was removed with a rotary evaporator, and the crude product was purified by column chromatography. Elution was conducted with mixtures of dichloromethane and methanol. The solvent was then evaporated to obtain PNDA as a dark yellow solid with a yield of 88%. ^1H NMR spectroscopy, (600 MHz, DMSO-d_6), δ (ppm): 7.46−7.43 (t, 2H), 7.33−7.30 (t, 1H), 7.13−7.11 (d, 2H), 6.94−6.89 (dd, 1H, j = 9.01 Hz), 6.67−6.63 (dd, 1H, j = 8.94 Hz), 6.42−6.36 (m, 2H, j = 5.57 Hz), 5.98−5.93 (m, 2H, j = 4.51 Hz), 3.73−3.69 (m, 1H, j = 4.75 Hz), 3.05−3.01 (m, 1H, j = 4.73 Hz), 2.83−2.81 (d, 1H), 2.63−2.61 (d, 1H), 1.71−1.66 (t, 2H), 1.43−1.21 (m, 4H, j = 6.22 Hz) (Figure S4). ^{13}C NMR spectroscopy, (600 MHz, DMSO-d_6), δ (ppm): 165.9, 149.1, 132.2, 131.5, 130.3, 129.4, 128.8, 126.6, 120.9, 60.2, 59.9, 28.7, 28.4, 23.9, 23.6 (Figure S5). ^{31}P NMR spectroscopy, (600 MHz, DMSO-d_6), δ (ppm): 7.47 (s) (Figure S6). Calcd for $C_{18}H_{21}N_2O_4P$ 361.1311 $[M + H]^+$, found 361.1865.

2.5. Synthesis of 1,4-Phenylene diacrylate (1,4-PhDA). Hydroquinone (10.00 g, 98.9 mmol, 1.0 equiv) and triethylamine (25.01 g, 247.3 mmol, 2.5 equiv) were dissolved in dry dichloromethane (300 mL), and the solution was cooled to 0 °C in an ice bath. A solution of acryloyl chloride (19.69 g, 217.6 mmol, 2.2 equiv) in dry dichloromethane (50 mL) was added dropwise over 30 min at 0 °C. The mixture was then allowed to gradually warm up to 25−30

https://doi.org/10.1021/acs.macromol.4c01288
Macromolecules 2024, 57, 9396−9407

°C and stirred for an additional 12 h. Then, the mixture was extracted twice with water, and the organic layer was collected and dried over Na_2SO_4. The solvent was removed under reduced pressure, and the crude product was purified by column chromatography. The elution was conducted with 100% dichloromethane. The solvent was removed with a rotary evaporator to obtain 1,4-phenylene diacrylate (1,4-PhDA) as a light yellow solid with a yield of 75%. ^{1}H NMR spectroscopy, (600 MHz, $CDCl_3$), δ (ppm): 7.16 (phenyl, s, 4H), 6.60 (dd, 2H, ^2J = 10.5 Hz, ^3J = 27.8 Hz), 6.32 (dd, 2H, ^3J = 17.3 Hz, ^3J = 27.8 Hz), 6.01 (dd, 2H, ^2J = 10.5 Hz, ^3J = 17.3 Hz) (Figure S7). ^{13}C NMR spectroscopy, (600 MHz, $CDCl_3$), δ (ppm): 164.4, 148.0, 132.8, 127.7, 124.4 (Figure S8).

2.6. General Procedure of Preparation of Polyphosphorodiamidates by Michael Addition with Dithiols (PN1−PN7). Solutions of PNDA (600 mg, 1.67 mmol, 1.0 equiv) and various amounts of dithiols and/or 1,4-phenyl diacrylate (see Table S1) were dissolved in 2.0 mL of anhydrous DMF and placed in 25 mL round-bottom flasks. Then, the mixtures were bubbled with nitrogen for 15 min. Afterward, the reaction flasks were placed in an oil bath at 100 °C under a nitrogen atmosphere and stirred for 24 h. After polymerization, the reaction mixtures were cooled to 25−30 °C. The products were then precipitated into 10 mL methanol, centrifuged, and the pellets were then dissolved in 2 mL of DMF and reprecipitated in methanol again twice. Finally, the products were dried in a vacuum oven at 60 °C for 24 h.

PN1 ^{1}H NMR spectroscopy, (600 MHz, DMSO-d_6), δ (ppm): 7.47−7.29 (m, Ar−H), 3.55 (m), 3.30 (m), 3.04 (m), 2.93 (m), 2.78 (m), 2.67 (m), 1.66 (m), 1.34 (m), 1.35 (m), 1.01 (m) (Figure S9). ^{31}P NMR spectroscopy, (600 MHz, DMSO-d_6), δ (ppm): 7.74 (s) (Figure S10).

PN2 ^{1}H NMR spectroscopy, (600 MHz, DMSO-d_6), δ (ppm): 7.74−7.20 (m, Ar−H), 3.62 (m), 3.04 (m), 2.79 (m), 2.61 (m), 1.65 (m), 1.35 (m), 1.18 (m), 0.99 (m) (Figure S11). ^{31}P NMR spectroscopy, (600 MHz, DMSO-d_6), δ (ppm): 7.74 (s) (Figure S12).

PN3 ^{1}H NMR spectroscopy, (600 MHz, DMSO-d_6), δ (ppm): 7.57−6.62 (m, Ar−H), 4.07 (br), 3.79 (m), 3.53 (br, m), 3.12−2.42 (br, m), 1.82−0.87 (br, m) (Figure S13). ^{31}P NMR spectroscopy, (600 MHz, DMSO-d_6), δ (ppm): 7.78 (s) (Figure S14).

PN4 ^{1}H NMR spectroscopy, (600 MHz, DMSO-d_6), δ (ppm): 7.57−6.67 (m, Ar−H), 4.07 (br), 3.79 (m), 3.53 (br, m), 3.12−2.42 (br, m), 1.82−0.87 (br, m) (Figure S15). ^{31}P NMR spectroscopy, (600 MHz, DMSO-d_6), δ (ppm): 7.76 (s) (Figure S16).

PN5 ^{1}H NMR spectroscopy, (600 MHz, DMSO-d_6), δ (ppm): 7.53−6.95 (m, Ar−H)), 3.53 (br, m), 3.12−2.42 (br, m), 1.82−0.87 (br, m) (Figure S17). ^{31}P NMR spectroscopy, (600 MHz, DMSO-d_6), δ (ppm): 7.44 (s) (Figure S18).

PN6 ^{1}H NMR spectroscopy, (600 MHz, $CDCl_3$-d_1), δ (ppm): 7.23−6.92 (m, Ar−H), 4.67 (br), 3.53 (br), 3.32 (br), 1.60 (br), 1.34 (br), 1.14 (br), 0.94 (br), 0.79 (br) (Figure S19). ^{31}P NMR spectroscopy, (600 MHz, $CDCl_3$−d_1), δ (ppm): 7.59 (s) (Figure S20).

PN7 ^{1}H NMR spectroscopy, (600 MHz, DMSO-d_6), δ (ppm): 7.78−7.19 (m, Ar−H), 7.15 (m), 6.75 (m), 5.21 (s), 5.06 (s), 4.92 (s), 4.38 (br), 3.50 (br), 1.75−1.63 (m−br), 1.28−1.02 (br) (Figure S21). ^{31}P NMR spectroscopy, (600 MHz, DMSO-d_6), δ (ppm): 7.22 (s) (Figure S22).

2.7. General Procedure of Preparation of Polyphosphorodiamidates by Aza-Michael polyaddition (PN8−PN9). PNDA (600 mg, 1.67 mmol, 1.0 equiv) and various amounts of amines (see Table S1) in 2.0 mL of anhydrous DMF were placed in 25 mL round-bottom flasks. Then, the mixtures were bubbled with nitrogen for 15 min. Afterward, the reaction flasks were placed in an oil bath at 100 °C under a nitrogen atmosphere and stirred for 24 h. After polymerization, the reaction mixtures were cooled to 25−30 °C. The products were then precipitated into 10 mL methanol, centrifuged, and the pellets were then dissolved in 2 mL of DMF and reprecipitated in methanol again twice. Finally, the products were dried in a vacuum oven at 60 °C for 24 h.

PN8 ^{1}H NMR spectroscopy, (600 MHz, DMSO-d_6), δ (ppm): 7.38−7.11 (m, Ar−H), 7.06 (m, Ar−H), 6.57−6.51 (m, Ar−H), 3.54 (m), 2.99−2.77 (m), 1.61 (m), 1.32 (m), 1.13 (m), 0.95 (m) (Figure S23). ^{31}P NMR spectroscopy, (600 MHz, DMSO-d_6), δ (ppm): 7.63 (s) (Figure S24).

PN9 ^{1}H NMR spectroscopy, (600 MHz, DMSO-d_6), δ (ppm): 7.47−7.29 (m, Ar−H), 7.16−7.13 (m, Ar−H), 3.54 (m), 2.99−2.77 (m), 1.61 (m), 1.32 (m), 1.13 (m), 0.95 (m) (Figure S25). ^{31}P NMR spectroscopy, (600 MHz, DMSO-d_6), δ (ppm): 8.05 (m),−5.26 (s),−16.57 (s) (Figure S26).

2.8. General Procedure for the Synthesis of Polyphosphorodiamidates by Radical Thiol-ene Polyaddition (PN1*−PN7*). PNDA (600 mg, 1.67 mmol, 1.0 equiv), various amounts of dithiols and/or 1,4-phenyl diacrylate (see Table S2), and ABCN (8.16 mg, 0.033 mmol, 0.02 equiv) were dissolved in 2.0 mL of anhydrous DMF and placed in 25 mL round-bottom flasks (see Table S2). Then, the mixtures were bubbled with nitrogen for 15 min. Afterward, the reaction flasks were placed in an oil bath at 100 °C under a nitrogen atmosphere and stirred for 24 h. After polymerization, the reaction mixtures were cooled to 25−30 °C. The products were then precipitated into 10 mL methanol, centrifuged, and the pellets were then dissolved in 2 mL of DMF and reprecipitated in methanol again twice. Finally, the products were dried in a vacuum oven at 60 °C for 24 h.

PN1* ^{1}H NMR spectroscopy, (600 MHz, DMSO-d_6), δ (ppm): 7.47−7.29 (m, Ar−H), 3.55 (m), 3.30 (m), 3.04 (m), 2.93 (m), 2.78 (m), 2.67 (m), 1.66 (m), 1.34 (m), 1.35 (m), 1.01 (m) (Figure S27).

PN2* ^{1}H NMR spectroscopy, (600 MHz, DMSO-d_6), δ (ppm): 7.74−7.20 (m, Ar−H), 3.62 (m), 3.04 (m), 2.79 (m), 2.61 (m), 1.65 (m), 1.35 (m), 1.18 (m), 0.99 (m) (Figure S28).

PN3* ^{1}H NMR spectroscopy, (600 MHz, DMSO-d_6), δ (ppm): 7.57−6.62 (m, Ar−H), 4.07 (br), 3.79 (m), 3.53 (br, m), 3.12−2.42 (br, m), 1.82−0.87 (br, m) (Figure S29).

PN4* ^{1}H NMR spectroscopy, (600 MHz, DMSO-d_6), δ (ppm): 7.57−6.67 (m, Ar−H), 4.07 (br), 3.79 (m), 3.53 (br, m), 3.12−2.42 (br, m), 1.82−0.87 (br, m) (Figure S30).

PN5* Cross-linked

PN6* ^{1}H NMR spectroscopy, (600 MHz, $CDCl_3$), δ (ppm): 7.23−6.92 (m, Ar−H), 4.67 (br), 3.53 (br), 3.32 (br), 1.60 (br), 1.34 (br), 1.14 (br), 0.94 (br), 0.79 (br) (Figure S31).

FPN7* ^{1}H NMR spectroscopy, (600 MHz, DMSO-d_6), δ (ppm): 7.78−7.19 (m, Ar−H), 7.15 (m), 6.75 (m), 5.21 (s), 5.06 (s), 4.92 (s), 4.38 (br), 3.50 (br), 1.75−1.63 (m-br), 1.28−1.02 (br) (Figure S32).

2.9. Preparation of Polyphosphorodiamidates by Photopolymerization (PN10−PN13). A solution of PNDA (50 mg, 0.139 mmol, 1.0 equiv) and TADT (38 mg, 0.139 mmol, 1.0 equiv for PN10) or TADT (57 mg, 0.208 mmol, 1.5 equiv for PN11) or DMTD (21 mg, 0.139 mmol, 1.0 equiv for PN12) or DMTD (31 mg, 0.208 mmol, 1.5 equiv for PN13) and DMPA (25 mg, 0.097 mmol, 0.7 equiv) was dissolved in 1.0 mL anhydrous DMF in glass vials, which were sealed with a rubber septum, followed by purging with nitrogen for 5−10 min. Afterward, the reaction flasks were stirred and placed in a UV LED curing system (Awellcure, 365 nm, 4 mW·cm^{-2}) for 15 min. The products were then precipitated into 2 mL of methanol and centrifuged, and the pellets were then dissolved in 0.5 mL of DMF and reprecipitated in methanol again twice. Finally, the products were dried in a vacuum oven at 60 °C for 24 h.

2.10. Synthesis of Bis((2-oxo-1,3-dioxolan-4-yl)methyl) Phenyl Phosphate (PP). Diphenyl phosphorochloridate (2000 mg, 9.90 mmol, 1.0 equiv) was dissolved in dry dichloromethane (10 mL), and the solution was cooled to 0 °C in an ice bath. A solution of glycerol 1,2-carbonate (2,572 mg, 21.78 mmol, 2.2 equiv) and triethylamine (2,500 mg, 24.75 mmol, 2.5 equiv) in dry dichloromethane (10 mL) was added dropwise over 30 min at 0 °C. The mixture was then allowed to gradually warm up to 25−30 °C and stirred for an additional 12 h. Then, the mixture was extracted with water, and the organic layer was collected and dried over Na_2SO_4. The solvent was removed under reduced pressure, and the crude product was purified by column chromatography. Elution was

https://doi.org/10.1021/acs.macromol.4c01288
Macromolecules 2024, 57, 9396−9407

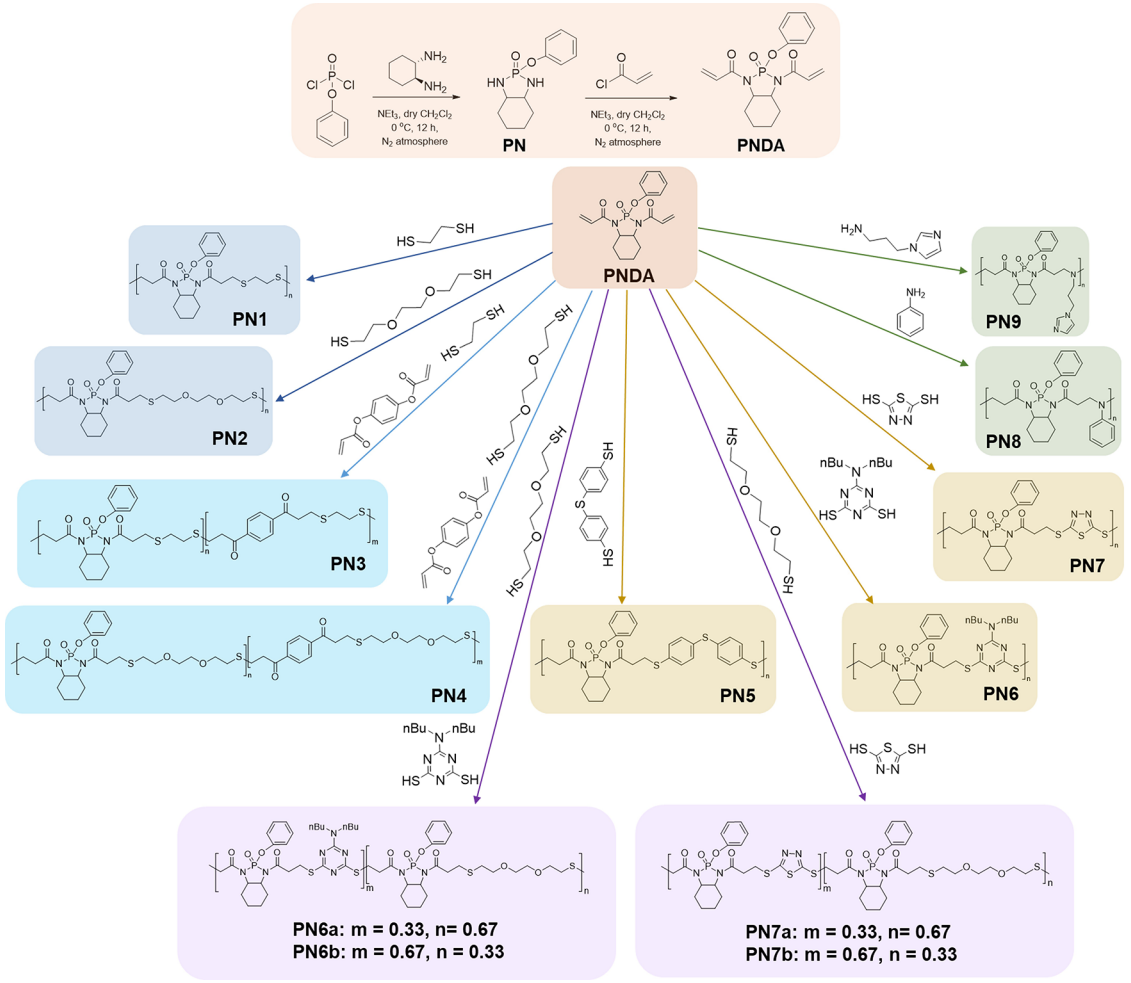

Figure 1. Synthetic route for obtaining 1,1'-(2-oxido-2-phenoxyhexahydrobenzo[d][1,3,2]diazaphosphole-1,3-diyl)bis(prop-2-en-1-one) (PNDA) and Michael addition or radical thiol-ene polyaddition of PNDA with different dithiols and amines.

conducted with mixtures of dichloromethane and methanol. The solvent was removed with a rotary evaporator to obtain PP as a viscous transparent oil with a yield of 52%. ^{1}H NMR spectroscopy, (600 MHz, DMSO-d_6), δ (ppm): 7.43−7.40 (t, 2H), 7.27−7.25 (t, 1H), 7.23−7.20 (dd, 2H), 5.06 (br, 2H), 4.59−4.56 (m, 2H), 4.46−4.42 (m, 2H), 4.31−4.25 (m, 2H) (Figure S33). ^{13}C NMR spectroscopy, (600 MHz, DMSO-d_6), δ (ppm): 160.0, 150.3, 130.5, 126.1, 120.4, 75.0, 67.9, 66.0 (Figure S34). ^{31}P NMR spectroscopy, (600 MHz, DMSO-d_6), δ (ppm): −6.51 (s) (Figure S35).

2.11. Preparation of Polyhydroxyurethanes. A solution of PP (50 mg, 0.133 mmol, 1.0 equiv) and HMDA (15 mg, 0.133 mmol, 1.0 equiv for PHU1) or *m*-XDA (18 mg, 0.133 mmol, 1.0 equiv for PHU2) in 1.0 mL of anhydrous DMSO was placed separately in 10 mL round-bottom flasks. Then, the mixtures were bubbled with nitrogen for 15 min. Afterward, the reaction flasks were placed in an oil bath at 25 °C under a nitrogen atmosphere and stirred for 18 h. After polymerization, the reaction mixtures were cooled to 25−30 °C. The products were then precipitated into 10 mL ethyl acetate, centrifuged, and the pellets were then dissolved in 0.5 mL of DMSO and reprecipitated in ethyl acetate again twice. Finally, the products were dried in a vacuum oven at 40 °C for 24 h.

PHU1 ^{1}H NMR spectroscopy, (600 MHz, DMSO-d_6), δ (ppm): 7.44−7.36 (br, 2H), 7.32−7.20 (br, 2H), 7.16−7.13 (t, 2H), 6.75−6.74 (dd, 3H), 4.56−3.31 (br, m), 2.95 (br), 2.70−2.67 (t), 1.50−1.22 (m) (Figure S36).

PHU2 ^{1}H NMR spectroscopy, (600 MHz, DMSO-d_6), δ (ppm): 7.16−7.13 (t, 2H), 6.75−6.74 (dd, 3H), 4.90, 4.79, 4.58, 4.48, 4.37, 4.29, 4.18, 3.9, 3.67, 3.52 (Figure S37).

2.12. Preparation of the Epoxy Thermosets. Solutions of 20 g of polymer additives in 20−30 mL of dichloromethane were thoroughly mixed with 150 g of diglycidyl ether of bisphenol. Then, 52.5 g of 2,2′-dimethyl-4,4′-methylene-bis(cyclohexylamine) was added, and the mixture was slowly stirred with a wooden spatula until it was homogeneous. The mixture was poured in a silicone mold, and bubbles were removed in vacuum. The mixtures were cured in an oven at 120 and 150 °C for 1 h. Control samples without polymer additives were prepared by the same method. Samples for UL-94 and LOI measurements were then cut into specified dimensions following EN 60695-11-10 and ASTM D2863 standards, respectively, and stored in a desiccator for at least 48 h.

3. RESULTS AND DISCUSSION

PNDA, a new monomer, was synthesized by the reaction between phenyl phosphorodichloridate and *trans*-1,2-diaminocyclohexane, followed by a reaction with acryloyl chloride to form phosphorodiamidate bonds (see Figure 1). The chemical structure of PNDA was confirmed by ^{1}H, ^{13}C, and ^{31}P NMR spectroscopies (Figures S1−S6). Polymers were then synthesized by Michael addition reactions between PNDA and various dithiols or amines in the presence and absence of a radical initiator (Figure 1). Additionally, polymers were synthesized by thiol-ene photopolymerizations. The thiol-ene polyaddition was evidenced by a reduction of the protons of signals associated of protons of the double bonds of PNDA in

https://doi.org/10.1021/acs.macromol.4c01288
Macromolecules 2024, 57, 9396−9407

Table 1. Comparison of Diffusion Coefficient (D) and Apparent Average Molecular Weight (M_w) of Polyphosphorodiamidates Synthesized by Michael Addition (PN1−PN7), Aza-Michael Addition (PN8−PN9), and Radical Thiol-ene Polyaddition (PN1*−PN7*) Was Determined by ^{1}H DOSY NMR Spectroscopy[a]

Michael and aza-Michael addition	D ($m^2 \cdot s^{-1}$)	M_w ($g \cdot mol^{-1}$)	radical thiol-ene polyaddition	D ($m^2 \cdot s^{-1}$)	M_w ($g \cdot mol^{-1}$)	T_g (°C)
PN1	3.32×10^{-11}	35,750	PN1*	1.03×10^{-10}	8750	−9
PN2	5.70×10^{-11}	8750	PN2*	1.25×10^{-10}	5250	−17
PN3	6.62×10^{-11}	5950	PN3*	9.20×10^{-11}	11,600	104
PN4	6.64×10^{-11}	5900	PN4*	1.11×10^{-10}	7100	103
PN5	9.57×10^{-11}	2300	PN5*	cross-linked		57
PN6	7.06×10^{-11}	5000	PN6*	3.11×10^{-10}	500	65
			PN6a*	1.39×10^{-10}	3950	−8
			PN6b*	2.19×10^{-10}	1200	−5
PN7	7.57×10^{-11}	4200	PN7*	3.37×10^{-10}	400	95
			PN7a*	8.51×10^{-11}	14,300	13
			PN7b*	9.77×10^{-11}	9950	8
PN8	1.26×10^{-10}	5100				34
PN9	8.73×10^{-11}	13,400				79

[a]Glass transition temperatures (T_g) of the synthesized polyphosphorodiamidates were also measured.

^{1}H NMR spectra (δ = 5.9−6.9 ppm), with conversions exceeding >98% (Figures S9−S32).

Polyphosphodiamidates, incorporating aromatic rings, alkyl chains, phosphorus, nitrogen, and sulfur, can interact with size exclusion chromatography (SEC) columns via adsorption, electrostatic, or hydrophobic mechanisms. Thus, adsorption, influenced by van der Waals forces, hydrogen bonding, and $\pi-\pi$ interactions (especially from aromatic rings), can occur. Hydrophobic effects can also contribute to retention, particularly in aqueous mobile phases. Because of the tendency of the polymers to attach to columns, their molecular weights were estimated by ^{1}H DOSY NMR spectroscopy (see Table 1). With this method, the diffusion coefficients of the polymers are compared to diffusion coefficients of polymers with known molecular weights used for calibration (see Table S3).[46−48] Log/log curves of the weight-average molecular weights of PMMA standards were linear with diffusion coefficients of PMMA in DMSO-d_6 (see Table S3 and Figure S38).

We observed an almost conversion of PNDA in the ^{1}H NMR spectra of the polymers before purification (see Figure S39).[49] Indeed, ^{1}H NMR spectroscopy revealed the absence of unreacted acrylic protons in PNDA at chemical shifts (δ = 6.91 (1H), 6.65 (1H), 6.39 (2H), and 5.96 (2H) ppm) and the absence of unreacted acrylic protons in 1,4-phenyl acrylate at chemical shifts (δ = 6.55 (2H), 6.42 (2H), and 6.16 (2H) ppm). The apparent average molecular weight (M_w) of polyphosphorodiamidates (PN1−PN7) synthesized by Michael addition was determined by ^{1}H DOSY NMR spectroscopy and is listed in Table 1. The absence of insoluble PNDA homopolymer formation indicates that no cross-linking occurred during the reaction with dithiols. Furthermore, the absence of PNDA's characteristic acrylate proton signals (δ = 6.91, 6.65, 6.39, and 5.96 ppm) in the ^{1}H NMR spectrum (see Figure S40) confirms the absence of PNDA homopolymerization. The latter would have occurred in the case where only one bond of PNDA would have radically polymerized.

Polymerization of PNDA synthesized with aliphatic dithiols monomers without ABCN resulted in higher molecular weights (M_w = 5900−35,750 g mol^{-1}) compared with aromatic dithiols (M_w = 2300−5000 g mol^{-1}) after 24 h of polymerization due to poorer nucleophilicity of aromatic thiols.[50,51] However, when 1,4-phenylene diacrylate, an aromatic diacrylic comonomer, was added to form terpolymers with PNDA and either 1,2-ethanedithiol (PN3) or with 2,2'-(ethylenedioxy) diethanethiol (PN4) at a molar ratio of 0.25:0.25:0.50, the terpolymers displayed lower molecular weights compared to the copolymer of PN1 and PN2 (see Table 1). The enhanced electron-withdrawing effect around the C═C bond in PNDA, due to the presence of phosphorus, oxygen, and the aromatic ring, is stronger than that of the C═C bond in 1,4-phenylene diacrylate. This greater electron-withdrawing effect contributes to PNDA's remarkably fast polymerization rate. The thiolate, a potent nucleophile, readily attacks the activated C═C bond at the electrophilic β-carbon, forming an intermediate carbon-centered anion (or enolate). This strong base then abstracts a proton from a thiol, yielding the thiol-ene product with regioselective anti-Markovnikov formation.[52−54] Due to the high conversion (near 100%) achieved during the polymerization of PN3 and PN4 and the fact that ^{1}H DOSY NMR spectra of the two polymers (see Figures S41 and S42) showed one coefficient of diffusion, the composition of the polymers was related to the monomer feed ratio.

We investigated the molecular weight of copolymers formed with aniline as a representative of aromatic amines (PN8) and 1-(3-aminopropyl)imidazole (PN9). The latter molecule contains a heterocyclic imidazole ring, which is suitable for application as a flame retardant.[55] These copolymers were then compared to those synthesized by using dithiols. The molecular weights of the amine comonomers, PN8 and PN9, were 5100 and 13,400 g mol^{-1}, respectively. The higher molecular weight of the aliphatic amine can be attributed to its higher reactivity and lower steric hindrance in comparison to the aromatic amine.

Molecular weight comparisons between PN1*−PN2* and PN6*−PN7* synthesized with ABCN were generally lower than those synthesized without ABCN. In the radical-mediated thiol-ene reaction, the initiator generates radicals that deprotonate thiols, producing thiyl radicals. These radicals then react with electron-rich alkenes to form thioether bonds.[52−54] In the anion-mediated pathway, a thiolate anion is formed, which reacts with electron-deficient alkenes to form a thioether bond.[52−54] The polarity of the solvent influences the reaction mechanism and molecular weight. Thus, the polar solvent DMF can stabilize thiolate anions, promoting the thiol-Michael reaction and potentially leading to higher molecular

https://doi.org/10.1021/acs.macromol.4c01288
Macromolecules 2024, 57, 9396−9407

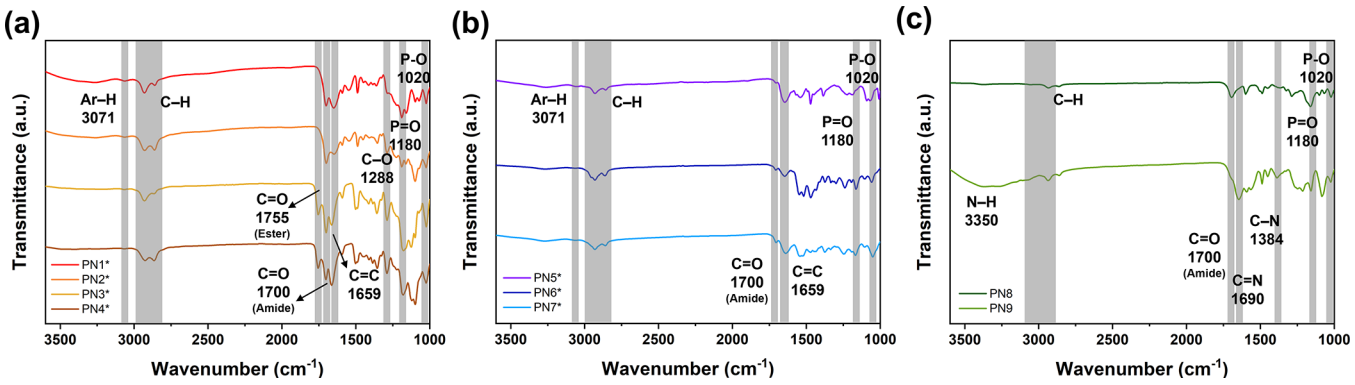

Figure 2. Fourier transform infrared (FT-IR) spectroscopy spectra of PN1*–PN4* (a), PN5*–PN7* (b), and PN8–PN9 (c).

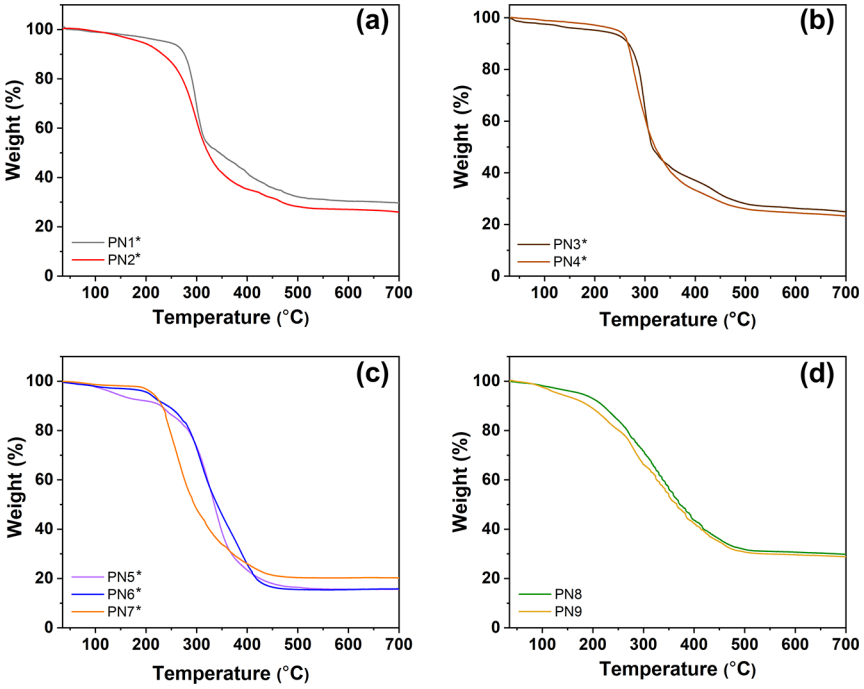

Figure 3. Thermograms of PN1*–PN2* (a), PN3*–PN5*, (b) PN6*–PN7*, (c), and PN8–PN9 (d).

weights.[56] In contrast, PN3*–PN4* synthesized with ABCN exhibited higher molecular weights compared to PN3–PN4 synthesized without ABCN. This is because the electron density of the C═C bond in acrylate within 1,4-phenylene diacrylate is higher than that in PNDA, leading to an increased reactivity.

The polymers produced with PNDA and 4-(4-sulfanylphenyl)sulfanyl benzenethiol (PN5*) using radical thiol-ene polyaddition were not soluble in common organic solvents such as toluene, chlorobenzene, DMF, THF, chloroform, and dimethyl sulfoxide. Yao et al. reported that thiol-yne polymerization with 4-(4-sulfanylphenyl)sulfanyl benzenethiol monomers in toluene and DMF also yielded insoluble polymers.[57]

We attributed the low molecular weight of polymers formed with TADA (PN6*) and DMTD (PN7*) comonomers to the equilibrium between their thiol and thioamide tautomers, reducing the availability of reactive thiol groups for polymerization (see Figure S43).[58,59] In this case, solubility issues did not hinder the analysis of these samples (see Table S4). Finally, we determined the solubility of standard PMMAs and PNs in THF, DMF, DMSO, and $CHCl_3$, as detailed in Table S4.

To increase the molecular weight, we copolymerized EDDT with TADA (PN6a* and PN6b*) and DMTD (PN7a* and PN7b*) at different ratios (see Figure 1). After terpolymerization with EDDT, the molecular weights of PN6a* (3950 g·mol^{-1}), PN6b* (1200 g·mol^{-1}), PN7a* (14,300 g·mol^{-1}), and PN7b* (9950 g·mol^{-1}) were higher due to the higher reactivity of aliphatic dithiols. Tentative trials to increase molecular weights of polymers synthesized with TADA and DMTD by photopolymerization with DMPA as the photoinitiator were unsuccessful (see Table S5).

The glass transition temperatures (T_g) of the PNs polymers were measured by differential scanning calorimetry (DSC) (see Table 1 and Figures S44–S56). Polymers of PNDA monomer and aliphatic thiols produced polymers with T_gs lower than room temperature (PN1* and PN2*), which could be increased to ∼103–104 °C upon terpolymerization with 1,4-phenylene diacrylate (PN3* and PN4*). Polymers prepared with aromatic thiols led to more rigid polymers with T_gs between 57 and 95 °C (PN5*–PN7*). Copoly-

https://doi.org/10.1021/acs.macromol.4c01288
Macromolecules 2024, 57, 9396–9407

merization with aromatic amines also led to an increase of polymer rigidity, consequently increasing the T_gs from 34 °C for PN8 to 79 °C for PN9.

Characteristic absorption peaks of P═O and P−O stretching vibrations were observed at 1180 and 1020 cm^{-1} in the Fourier transform infrared (FT-IR) spectrometer spectra of the polymers (see Figure 2), respectively. Meanwhile, signals associated with C−H, C═C (in aromatic ring), and Ar−H were detected at 2928, 1659, and 3071 cm^{-1}, respectively. Additionally, stretching vibrations of C═O (ester and amide bonds) were detected in 1755 and 1700 cm^{-1} for PN1−PN4, while stretching vibrations of C═N, C−N were observed at 1690 and 1384 cm^{-1} for PN8 and PN9. Interestingly, the N−H stretching vibration at 3350 cm^{-1} related to the amino group of PN9 indicated the conversion of primary amine groups in 1-(3-aminopropyl)imidazole to secondary amine groups.

The thermal stability of the polymers was investigated by thermal gravimetry analysis (TGA) (Figure 3, Table S6). Aliphatic dithiol-based polymers (PN1* and PN2*) exhibited a single-step decomposition at 299 °C (Figure 3a). The initial decomposition steps observed for PN3 and PN4 are similar to the ones observed for PN1*−PN2*. However, these polymers (PN1*−PN4*) showed an increase in the decomposition rate between 330 and 380 °C (Figure 3a,b). This is probably due to the breakdown of the aromatic units present in the copolymers. In contrast, polymers synthesized with aromatic dithiols (PN5*−PN7*) or amines (PN8−PN9) exhibited a broader decomposition profile, decomposing over a wider temperature range from 200 to 450 °C (Figure 3c,d). PN1−4, PN8, and PN9 contained higher density of phosphorus, sulfur, and nitrogen atoms compared with hyperbranched polyphosphorodiamidates,[28] leading to a higher residue yield (up to 30 wt % in our work against 11−18 wt % in the literature[28]). A higher production of residue char is beneficial for flame retardant applications. Indeed, the char layer during combustion serves to protect materials against heat and slows the diffusion of oxygen in the flame zone.[1,28,35] The protective char layer acts as a barrier, reducing the spread of fire and enhancing the materials fire resistance.[1,28,35]

XPS can be used to examine the chemical structure of polymers. Elemental compositions of the polymers were measured by X-ray photoelectron spectroscopy (XPS, Table 2, Figures S57−S61). The C_{1s} spectra (Figure S57) revealed the presence of three binding energies: 284.5 eV for C−H or C−C bonds, 286.0 eV for C−O groups, and 287.8 eV for C═O bonds. Furthermore, two discernible binding energies at 531.5 and 532.5 eV assigned to −O−groups within P−O−C bonds and C═O groups in phosphorodiamidates or carbonyl compounds were observed in the O_{1s} spectra (see Figure S58). In the N_{1s} spectra, four binding energies at 398.4, 399.0, 399.7, and 400.1 eV were detected, corresponding to N═N, sp^2-hybridized nitrogen C−N═C bonds, N−C═O bonds, and C−N−H (positive charge localization in heterocycles), respectively (Figure S59).[60,61] The S_{2p} spectra (Figure S60) featured two signals with 163.6 and 164.0 eV, which were assigned to the C−S−C bond and S−C═N or S−C═C bond, respectively. The P_{2p} XPS spectra (Figure S61) contained peaks at 132.7, 133.5, and 134.4 eV, which corresponded to P−N, P═O, and P−O bonds, respectively. This is because the binding energies of P−C coordination bonds (131.2−132.2 eV) were lower than that of P−N and P−O bonds.[62] The contents of each element in the polymers were similar to the theoretical contents calculated according to the expected structures of the polymers (Table 2).

Table 2. Comparisons of the Theoretical Contents of C, O, N, S, and P Atoms in the Polymers and the Contents Measured by X-ray Photoelectron Spectroscopy

	C (at %)		O (at %)		N (at %)		S (at %)		P (at %)	
entry	th.	exp.	th.	exp.	th.	exp.	th.	exp.	th.	exp.
PN1*	69	68	14	16	7	6	7	6	3	5
PN2*	69	67	17	16	6	5	6	5	3	3
PN3*	69	68	16	13	7	6	8	10	2	4
PN4*	69	65	20	19	3	5	7	8	2	3
PN5*	75	81	10	8	5	4	8	7	3	2
PN6*	69	76	10	7	14	12	5	4	2	2
PN7*	63	75	13	9	13	9	9	5	3	2
PN8*	75	77	13	15	9	6			3	2
PN9*	71	77	12	15	15	6			3	2

Furthermore, we prepared polyhydroxyurethanes (PHUs) with phosphorus in their main chain. First, we synthesized a new monomer (PP) by the reaction between phenyl phosphorodichloridate and glycerol 1,2-carbonate (see Figure 4a). The chemical structure of PP was confirmed by ^1H, ^{13}C, and ^{31}P NMR spectroscopies (Figures S33−S35). PHUs were synthesized by ring-opening of cyclic carbonate with different amines (HMDA for PHU1 and *m*−XDA for PHU2) at 25 °C without catalysts. The ring-opening of cyclic carbonate in the PP monomer was evidenced by a reduction of the protons of signals in−CH of PP in ^1H NMR spectra (δ = 5.0 ppm), with conversions of 93% for PHU1 and 77% for PHU2 (Figures S36 and S37). PHU1 exhibits higher conversion compared to PHU2 due to the higher pK_a (11.86 at 20 °C) of HMDA used in its synthesis compared to the pK_a (9.77 at 25 °C) of *m*−XDA used for PHU2.[63,64] Higher pK_a leads to a stronger nucleophile, potentially leading to a more efficient ring-opening reaction in the PHU1 synthesis. PHU1 exhibited a significantly higher molecular weight (M_w = 14,200 g·mol^{-1}) compared to PHU2 (M_w = 4,800 g·mol^{-1}) (see Table S5). Characteristic absorption peaks of P═O and P−O stretching vibrations were observed at 1180 and 1020 cm^{-1}, respectively, in the Fourier transform infrared (FT-IR) spectra of the polymers (see Figure 4b). Meanwhile, signals associated with C−H and C═C (in aromatic ring) were detected at 2940 and 1540 cm^{-1}, respectively. Additionally, stretching vibrations of C═O (ester and amide bonds) were detected at 1700 and 1650 cm^{-1}. The presence of O−H and N−H stretching vibrations at 3320 cm^{-1} in the PHU spectra confirms the complete ring-opening reaction of the PP monomer with both HMDA and *m*-XDA in the main polymer chain. PHU2 exhibits higher decomposition temperatures compared to PHU1 (Figure 4c) due to the presence of more aromatic units in its main chain, as detailed in Table S6. However, both PHUs exhibited higher residue yields (up to 37 wt %) compared to PPDAs. This suggests that incorporation of the phosphorus moiety within the main chain of PHUs can enhance char formation during thermal degradation, leading to a higher residue yield.

Because of the high phosphorus content of the synthesized polymers, we investigated their properties as flame retardant additives in epoxy resins (EP). We selected PN−1* and PN−2* as additives due to their excellent miscibility with the EP matrix. A key parameter is the thermal stability of the resin in the presence of additives. The thermal stability of the epoxy

https://doi.org/10.1021/acs.macromol.4c01288
Macromolecules 2024, 57, 9396−9407

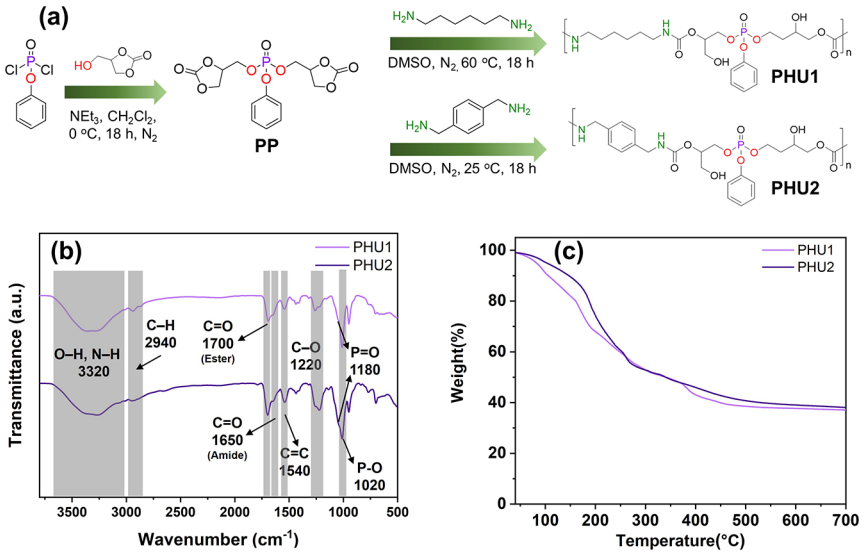

Figure 4. Synthetic route for obtaining bis((2-oxo-1,3-dioxolan-4-yl)methyl) phenyl phosphate (PP) and ring-opening polyaddition of PP with different amines (a), Fourier transform infrared (FT-IR) spectroscopy spectra of PHU1−2 (b), and thermograms of PHU1−2 (c).

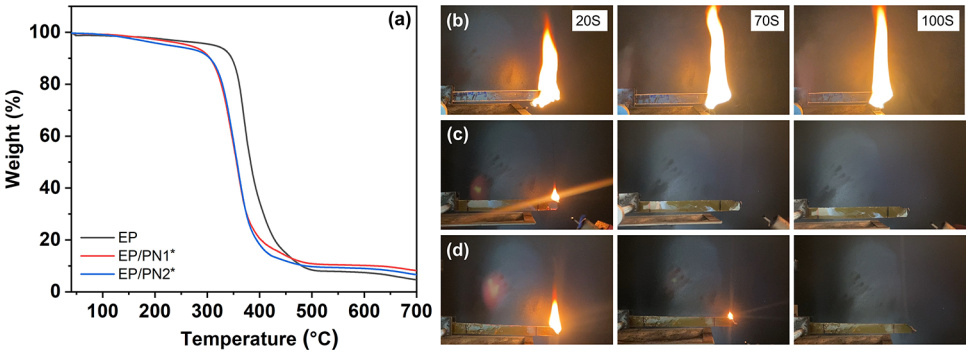

Figure 5. TGA thermograms (a) and photographs captured during the UL-94 horizontal tests for EP (b), EP/PN1* (c), and EP/PN2* (d) at 20, 70, and 100 s after the ignition source had been removed.

resins with 10 wt % additive was examined by TGA under nitrogen atmospheres (Figure 5a, Table S7). The pure epoxy resin was decomposed with a T_{max} at 372 °C, showing a single main step with a mass loss of 62 wt %. A shoulder appeared at 424 °C with another mass loss of 31 wt %, yielding 6 wt % residue at 700 °C. By comparison, the residue amount increased to ∼8 wt % in the presence of PN1* or PN2*. This enhanced char residue is expected to protect materials placed underneath from additional thermal oxidation and combustion.[65] Besides, the T_g of EP in the EP/PN1* composite increased by ∼5 °C with the addition of 10 wt % PN1 to epoxy, due to the rigid aromatic structure of PN1, whereas the T_g of EP in EP/PN2* decreased by ∼12 °C with 10 wt % PN2*, attributed to long aliphatic chains of PN2* (see Figure S62). The thermal decomposition profiles, residue yield, and T_g of EP/PN1* and EP/PN2* composites were similar to those observed for other polyphosphorodiamidate additives in epoxy resins.[28]

Flame retardancy of EP/PNs composites was evaluated by using the Limited Oxygen Index (LOI) and Underwriters Laboratories 94 (UL−94) tests. The LOI measures the minimum oxygen concentration a material needs to burn, with higher values indicating better flame resistance. UL−94 categorizes materials based on their burning behavior under controlled conditions. Pure EP exhibited flammability, with a low LOI of 19.9%. Incorporation of PN1* and PN2* as additives in the EP thermosets slightly increased their LOI values to around 21%, suggesting an improved resistance to ignition. Notably, all samples achieved HB classification in the UL−94 horizontal burning test, indicating slow burning behavior in the horizontal orientation. As shown in Figure 5b, pure EP burned more extensively compared to EP/PN1* (Figure 5c) and EP/PN2* (Figure 5d). Crucially, EP/PN1* and EP/PN2* self-extinguished within 60 and 79 s, respectively, after the ignition source was removed. This improvement was comparable to results obtained with hyperbranched polyphosphoramides, polyphosphorodiamidates, polyphosphoramidates, and polyphosphates synthesized via different chemistries, which showed similar LOI values at a similar additive loading (10 wt %).[28]

The flame retardancy of PN1* and PN2 was evaluated through burn tests and compared to that of the non-halogenated flame retardants bisphenol A bis(diphenyl phosphate) (BDP) and DOPI. PN1 and PN2 were incorporated into the same epoxy resin matrix at a 10 wt % loading, replicating conditions from previous work reporting the efficiency of BDP and DOPI.[28,66] BDP and DOPI exhibited LOI values of 24.0% and 25.0%, respectively, achieving an HB rating in the UL−94 test.[28,66] The flame retardancy of EP/PN1* and EP/PN2* therefore demonstrated

https://doi.org/10.1021/acs.macromol.4c01288
Macromolecules 2024, 57, 9396−9407

a comparable performance to these nonhalogenated benchmark flame retardants.

Halogenated flame retardants such as polybrominated diphenyl ethers, hexabromocyclododecanes and tetrabromobisphenol display a low biodegradability and hence tend to bioaccumulate.[67,68] These compounds and their toxic degradation products contaminate air, soil, and water, posing long-term risks, including endocrine disruption and reproductive harm.[67,68] Polyphosphorodiamidates (PNs) offer potential environmental benefits compared with halogenated flame retardants. Their P−N bonds are susceptible to hydrolysis, potentially leading to more rapid degradation and reduced persistence.[19,28,35] While toxicity assessments of PNs, including various phosphorus-containing functional groups, are ongoing, initial results from fungal and plant cell studies suggest lower toxicity compared to the commercial flame retardant tetrabromobisphenol A.[35]

4. CONCLUSIONS

We successfully synthesized phosphorus-containing polymers by thiol-ene polymerization with various thiols and aza-Michael addition with amines. A comprehensive analysis involves differential scanning calorimetry, thermal gravimetry analysis, and X-ray photoelectron spectroscopy. Incorporating aromatic units and rigid rings in the polymers improved their thermal stability and the glass transition temperature. Additionally, the high density of phosphorus atoms in the phosphorodiamidate monomers promoted char formation during pyrolysis. Polyhydroxyurethanes were synthesized by derivatizing unsaturated phosphoramidates to epoxides and subsequently to cyclic carbonates that were then reacted with diamines. Polyphosphorodiamidates-containing aliphatic dithiols were selected for their compatibility with epoxy resin. These materials exhibit promising flame retardant properties due to their high sulfur and phosphorus contents, which acted synergistically to suppress flammability within the epoxy matrix. Future efforts will be dedicated to enhancing compatibility of the polyphosphorodiamidates with other polymer's matrixes and investigate their degradability.

■ ASSOCIATED CONTENT

Supporting Information

The Supporting Information is available free of charge at https://pubs.acs.org/doi/10.1021/acs.macromol.4c01288.

Compositions used for preparing polymers by radical thiol-ene polyaddition; weight-average molecular weight (M_w); dispersity index (PDI); diffusion coefficient (D) of PMMA standards; apparent average molecular weight of the polymers obtained by photopolymerization; ^{1}H, ^{13}C, ^{31}P, and ^{1}H DOSY NMR spectra of monomers and polymers; linear calibration curve of diffusion coefficients of PMMA standards in DMSO-d_6; temperatures at 5 wt % weight loss ($T_{5\%}$); temperature at maximum weight loss rates (T_{max}); maximum weight loss rate (R); char residue (CY) of polyphosphorodiamidates, polyhydroxyurethans, EP, and EP/PNs; high resolution C (1s), O (1s), N (1s), S (2p), and P (2p) XPS spectra of PNs; and DSC thermograms of EP, EP/PN1*, EP/PN2*, and PNs (PDF)

■ AUTHOR INFORMATION

Corresponding Author

Daniel Crespy − *Department of Materials Science and Engineering, School of Molecular Science and Engineering, Vidyasirimedhi Institute of Science and Technology (VISTEC), Rayong 21210, Thailand;* orcid.org/0000-0002-6023-703X; Email: daniel.crespy@vistec.ac.th

Author

Nantawat Kaekratoke − *Department of Materials Science and Engineering, School of Molecular Science and Engineering, Vidyasirimedhi Institute of Science and Technology (VISTEC), Rayong 21210, Thailand*

Complete contact information is available at: https://pubs.acs.org/10.1021/acs.macromol.4c01288

Notes

The authors declare no competing financial interest.

■ ACKNOWLEDGMENTS

We thank the funding given by the Vidyasirimedhi Institute of Science and Technology (VISTEC).

■ REFERENCES

(1) Velencoso, M. M.; Battig, A.; Markwart, J. C.; Schartel, B.; Wurm, F. R. Molecular Firefighting—How Modern Phosphorus Chemistry Can Help Solve the Challenge of Flame Retardancy. *Angew. Chem., Int. Ed.* **2018**, *57* (33), 10450−10467.

(2) Monge, S.; Canniccioni, B.; Graillot, A.; Robin, J.-J. Phosphorus-Containing Polymers: A Great Opportunity for the Biomedical Field. *Biomacromolecules* **2011**, *12* (6), 1973−1982.

(3) Gomes Rodrigues, D.; Monge, S.; Pellet-Rostaing, S.; Dacheux, N.; Bouyer, D.; Faur, C. A New Carbamoylmethylphosphonic Acid-Based Polymer for the Selective Sorption of Rare Earth Elements. *Chem. Eng. J.* **2019**, *371*, 857−867.

(4) Liu, J.; Huang, W.; Pang, Y.; Yan, D. Hyperbranched Polyphosphates: Synthesis, Functionalization and Biomedical Applications. *Chem. Soc. Rev.* **2015**, *44* (12), 3942−3953.

(5) Ghorai, A.; Banerjee, S. Phosphorus-Containing Aromatic Polymers: Synthesis, Structure, Properties and Membrane-Based Applications. *Prog. Polym. Sci.* **2023**, *138*, No. 101646.

(6) Perego, M.; Seguini, G.; Arduca, E.; Nomellini, A.; Sparnacci, K.; Antonioli, D.; Gianotti, V.; Laus, M. Control of Doping Level in Semiconductors Via Self-Limited Grafting of Phosphorus End-Terminated Polymers. *ACS Nano* **2018**, *12* (1), 178−186.

(7) Macarie, L.; Ilia, G. Poly(Vinylphosphonic Acid) and Its Derivatives. *Prog. Polym. Sci.* **2010**, *35* (8), 1078−1092.

(8) Kaekratoke, N.; Flood, A.; Crespy, D. Homopolymers and Copolymers with Iminodiacetic Acid Chelating Units for Scale Inhibition. *Desalination* **2024**, *583*, No. 117643.

(9) Deng, M.; Kumbar, S. G.; Wan, Y.; Toti, U. S.; Allcock, H. R.; Laurencin, C. T. Polyphosphazene Polymers for Tissue Engineering: An Analysis of Material Synthesis, Characterization and Applications. *Soft Matter* **2010**, *6* (14), 3119−3132.

(10) Ni, Z.; Yu, H.; Wang, L.; Shen, D.; Elshaarani, T.; Fahad, S.; Khan, A.; Haq, F.; Teng, L. Recent Research Progress on Polyphosphazene-Based Drug Delivery Systems. *J. Mater. Chem. B* **2020**, *8* (8), 1555−1575.

(11) Steinbach, T.; Alexandrino, E. M.; Wahlen, C.; Landfester, K.; Wurm, F. R. Poly(Phosphonate)S Via Olefin Metathesis: Adjusting Hydrophobicity and Morphology. *Macromolecules* **2014**, *47* (15), 4884−4893.

(12) Steinbach, T.; Ritz, S.; Wurm, F. R. Water-Soluble Poly(Phosphonate)S Via Living Ring-Opening Polymerization. *ACS Macro Lett.* **2014**, *3* (3), 244−248.

(13) Steinbach, T.; Wurm, F. R. Poly(Phosphoester)S: A New Platform for Degradable Polymers. *Angew. Chem., Int. Ed.* **2015**, *54* (21), 6098−6108.
(14) Cankaya, A.; Steinmann, M.; Bülbül, Y.; Lieberwirth, I.; Wurm, F. R. Side-Chain Poly(Phosphoramidate)S Via Acyclic Diene Metathesis Polycondensation. *Polym. Chem.* **2016**, *7* (31), 5004−5010.
(15) Zhou, N.; Zhi, Z.; Liu, D.; Wang, D.; Shao, Y.; Yan, K.; Meng, L.; Yu, D. Acid-Responsive and Biologically Degradable Polyphosphazene Nanodrugs for Efficient Drug Delivery. *ACS Biomater Sci. Eng.* **2020**, *6* (7), 4285−4293.
(16) Radmanesh, F.; Tena, A.; Sudhölter, E. J. R.; Hempenius, M. A.; Benes, N. E. Nonaqueous Interfacial Polymerization-Derived Polyphosphazene Films for Sieving or Blocking Hydrogen Gas. *ACS Appl. Polym. Mater.* **2023**, *5* (3), 1955−1964.
(17) Zhang, S.; Wang, H.; Shen, Y.; Zhang, F.; Seetho, K.; Zou, J.; Taylor, J.-S. A.; Dove, A. P.; Wooley, K. L. A Simple and Efficient Synthesis of an Acid-Labile Polyphosphoramidate by Organobase-Catalyzed Ring-Opening Polymerization and Transformation to Polyphosphoester Ionomers by Acid Treatment. *Macromolecules* **2013**, *46* (13), 5141−5149.
(18) Zhao, W.; Wang, G.; Liu, J.; Ban, D.; Cheng, T.; Liu, X.; Li, Y.; Huang, Y. Synthesis, Structure−Property and Flame Retardancy Relationships of Polyphosphonamide and Its Application on Epoxy Resins. *RSC Adv.* **2017**, *7* (79), 49863−49874.
(19) Steinmann, M.; Wagner, M.; Wurm, F. R. Poly(Phosphorodiamidate)S by Olefin Metathesis Polymerization with Precise Degradation. *Chem. - Eur. J.* **2016**, *22* (48), 17329−17338.
(20) Ou, M.; Lian, R.; Li, R.; Cui, J.; Guan, H.; Liu, L.; Jiao, C.; Chen, X. Solvent-Free Synthesis of a Hyperbranched Polyphosphoramide Cocuring Agent and Its Application in Fire-Safe, Mechanically Strong, and Tough Epoxy Resin. *ACS Appl. Polym. Mater.* **2023**, *5* (8), 6504−6515.
(21) Fu, L.; Xiao, G.; Yan, D. Sulfonated Poly(Arylene Ether Sulfone)S with Phosphine Oxide Moieties: A Promising Material for Proton Exchange Membranes. *ACS Appl. Mater. Interfaces.* **2010**, *2* (6), 1601−1607.
(22) Misenan, M. S. M.; Hempelmann, R.; Gallei, M.; Eren, T. Phosphonium-Based Polyelectrolytes: Preparation, Properties, and Usage in Lithium-Ion Batteries. *Polymers* **2023**, *15* (13), 2920.
(23) Hofmann, A.; Rauber, D.; Wang, T.-M.; Hempelmann, R.; Kay, C. W. M.; Hanemann, T. Novel Phosphonium-Based Ionic Liquid Electrolytes for Battery Applications. *Molecules* **2022**, *27* (15), 4729.
(24) Pelosi, C.; Tinè, M. R.; Wurm, F. R. Main-Chain Water-Soluble Polyphosphoesters: Multi-Functional Polymers as Degradable Peg-Alternatives for Biomedical Applications. *Eur. Polym. J.* **2020**, *141*, No. 110079.
(25) Pelosi, C.; Constantinescu, I.; Son, H. H.; Tinè, M. R.; Kizhakkedathu, J. N.; Wurm, F. R. Blood Compatibility of Hydrophilic Polyphosphoesters. *ACS Appl. Bio Mater.* **2022**, *5* (3), 1151−1158.
(26) David, G.; Negrell-Guirao, C.; Iftene, F.; Boutevin, B.; Chougrani, K. Recent Progress on Phosphonate Vinyl Monomers and Polymers Therefore Obtained by Radical (Co)Polymerization. *Polym. Chem.* **2012**, *3* (2), 265−274.
(27) Horzum, N.; Muñoz-Espí, R.; Glasser, G.; Demir, M. M.; Landfester, K.; Crespy, D. Hierarchically Structured Metal Oxide/Silica Nanofibers by Colloid Electrospinning. *ACS Appl. Mater. Interfaces.* **2012**, *4* (11), 6338−6345.
(28) Battig, A.; Markwart, J. C.; Wurm, F. R.; Schartel, B. Hyperbranched Phosphorus Flame Retardants: Multifunctional Additives for Epoxy Resins. *Polym. Chem.* **2019**, *10* (31), 4346−4358.
(29) Singh, P.; Pandit, S.; Sinha, M.; Yadav, D.; Parthasarathi, R. Computational Risk Assessment of Persistence, Bioaccumulation, and Toxicity of Novel Flame-Retardant Chemicals. *J. Phys. Chem. A* **2023**, *127* (51), 10747−10757.
(30) Shan, H.; Yan, L.; Xu, B.; Wang, D.; Wu, M. Polyphosphamide Containing Triazine and Melamine Cyanurate for Flame-Retardant Pa6. *ACS Appl. Polym. Mater.* **2023**, *5* (7), 5322−5333.
(31) Battig, A.; Markwart, J. C.; Wurm, F. R.; Schartel, B. Sulfur's Role in the Flame Retardancy of Thio-Ether−Linked Hyperbranched Polyphosphoesters in Epoxy Resins. *Eur. Polym. J.* **2020**, *122*, No. 109390.
(32) Gaan, S.; Sun, G.; Hutches, K.; Engelhard, M. H. Effect of Nitrogen Additives on Flame Retardant Action of Tributyl Phosphate: Phosphorus−Nitrogen Synergism. *Polym. Degrad. Stab.* **2008**, *93* (1), 99−108.
(33) Levchik, G. F.; Grigoriev, Y. V.; Balabanovich, A. I.; Levchik, S. V.; Klatt, M. Phosphorus−Nitrogen Containing Fire Retardants for Poly(Butylene Terephthalate). *Polym. Int.* **2000**, *49* (10), 1095−1100.
(34) Vothi, H.; Nguyen, C.; Pham, L. H.; Hoang, D.; Kim, J. Novel Nitrogen−Phosphorus Flame Retardant Based on Phosphonamidate: Thermal Stability and Flame Retardancy. *ACS Omega* **2019**, *4* (18), 17791−17797.
(35) Markwart, J. C.; Battig, A.; Zimmermann, L.; Wagner, M.; Fischer, J.; Schartel, B.; Wurm, F. R. Systematically Controlled Decomposition Mechanism in Phosphorus Flame Retardants by Precise Molecular Architecture: P−O Vs P−N. *ACS Appl. Polym. Mater.* **2019**, *1* (5), 1118−1128.
(36) Liang, Y.; Sullivan, H. L.; Carrow, K.; Mesfin, J. M.; Korpanty, J.; Worthington, K.; Luo, C.; Christman, K. L.; Gianneschi, N. C. Inflammation-Responsive Micellar Nanoparticles from Degradable Polyphosphoramidates for Targeted Delivery to Myocardial Infarction. *J. Am. Chem. Soc.* **2023**, *145* (20), 11185−11194.
(37) Liang, Y.; Sun, H.; Cao, W.; Thompson, M. P.; Gianneschi, N. C. Degradable Polyphosphoramidate Via Ring-Opening Metathesis Polymerization. *ACS Macro Lett.* **2020**, *9* (10), 1417−1422.
(38) Nagarkar, A. A.; Crochet, A.; Fromm, K. M.; Kilbinger, A. F. M. Efficient Amine End-Functionalization of Living Ring-Opening Metathesis Polymers. *Macromolecules* **2012**, *45* (11), 4447−4453.
(39) Li, C.; Callahan, A. J.; Simon, M. D.; Totaro, K. A.; Mijalis, A. J.; Phadke, K.-S.; Zhang, G.; Hartrampf, N.; Schissel, C. K.; Zhou, M. Fully Automated Fast-Flow Synthesis of Antisense Phosphorodiamidate Morpholino Oligomers. *Nat. Commun.* **2021**, *12* (1), 4396.
(40) Wang, H.; Dong, M.; Khan, S.; Su, L.; Li, R.; Song, Y.; Lin, Y.-N.; Kang, N.; Komatsu, C. H.; Elsabahy, M.; et al. Acid-Triggered Polymer Backbone Degradation and Disassembly to Achieve Release of Camptothecin from Functional Polyphosphoramidate Nanoparticles. *ACS Macro Lett.* **2018**, *7* (7), 783−788.
(41) Wang, J.; Zhang, P.-C.; Lu, H.-F.; Ma, N.; Wang, S.; Mao, H.-Q.; Leong, K. W. New Polyphosphoramidate with a Spermidine Side Chain as a Gene Carrier. *J. Controlled Release* **2002**, *83* (1), 157−168.
(42) Ye, X.; Wang, Y.; Zhao, Z.; Yan, H. A Novel Hyperbranched Poly(Phosphorodiamidate) with High Expansion Degree and Carbonization Efficiency Used for Improving Flame Retardancy of App/Pp Composites. *Polym. Degrad. Stab.* **2017**, *142*, 29−41.
(43) Steinmann, M.; Wurm, F. R. Water-Soluble and Degradable Polyphosphorodiamidates Via Thiol-Ene Polyaddition. *Polym. Degrad. Stab.* **2020**, *179*, No. 109224.
(44) Haudum, S.; Lenhart, S.; Müller, S. M.; Tupe, D.; Naderer, C.; Dehne, T.; Sittinger, M.; Major, Z.; Griesser, T.; Brüggemann, O.; et al. Amino Acid-Based Polyphosphorodiamidates with Hydrolytically Labile Bonds for Degradation-Tuned Photopolymers. *ACS Macro Lett.* **2023**, *12* (6), 673−678.
(45) Movsisyan, M.; Heugebaert, T. S. A.; Dams, R.; Stevens, C. V. Safe, Selective, and High-Yielding Synthesis of Acryloyl Chloride in a Continuous-Flow System. *ChemSusChem* **2016**, *9* (15), 1945−1952.
(46) Gu, K.; Onorato, J.; Xiao, S. S.; Luscombe, C. K.; Loo, Y.-L. Determination of the Molecular Weight of Conjugated Polymers with Diffusion-Ordered Nmr Spectroscopy. *Chem. Mater.* **2018**, *30* (3), 570−576.
(47) Voorter, P.-J.; McKay, A.; Dai, J.; Paravagna, O.; Cameron, N. R.; Junkers, T. Solvent-Independent Molecular Weight Determination of Polymers Based on a Truly Universal Calibration. *Angew. Chem., Int. Ed.* **2022**, *61* (5), No. e202114536.
(48) Ruzicka, E.; Pellechia, P.; Benicewicz, B. C. Polymer Molecular Weights Via Dosy Nmr. *Anal. Chem.* **2023**, *95* (20), 7849−7854.

https://doi.org/10.1021/acs.macromol.4c01288
Macromolecules 2024, 57, 9396−9407

(49) Nair, D. P.; Podgórski, M.; Chatani, S.; Gong, T.; Xi, W.; Fenoli, C. R.; Bowman, C. N. The Thiol-Michael Addition Click Reaction: A Powerful and Widely Used Tool in Materials Chemistry. *Chem. Mater.* **2014**, *26* (1), 724−744.
(50) Gunay, U. S.; Cetin, M.; Daglar, O.; Hizal, G.; Tunca, U.; Durmaz, H. Ultrafast and Efficient Aza- and Thiol-Michael Reactions on a Polyester Scaffold with Internal Electron Deficient Triple Bonds. *Polym. Chem.* **2018**, *9* (22), 3037−3054.
(51) Long, K. F.; Wang, H.; Dimos, T. T.; Bowman, C. N. Effects of Thiol Substitution on the Kinetics and Efficiency of Thiol-Michael Reactions and Polymerizations. *Macromolecules* **2021**, *54* (7), 3093−3100.
(52) Lowe, A. B. Thiol-Ene "Click" Reactions and Recent Applications in Polymer and Materials Synthesis. *Polym. Chem.* **2010**, *1* (1), 17−36.
(53) Sutherland, B. P.; Kabra, M.; Kloxin, C. J. Expanding the Thiol−X Toolbox: Photoinitiation and Materials Application of the Acid-Catalyzed Thiol−Ene (Act) Reaction. *Polym. Chem.* **2021**, *12* (10), 1562−1570.
(54) Hoyle, C. E.; Lee, T. Y.; Roper, T. Thiol−Enes: Chemistry of the Past with Promise for the Future. *J. Polym. Sci., Part A: Polym. Chem.* **2004**, *42* (21), 5301−5338.
(55) Huo, S.; Yang, S.; Wang, J.; Cheng, J.; Zhang, Q.; Hu, Y.; Ding, G.; Zhang, Q.; Song, P.; Wang, H. A Liquid Phosphaphenanthrene-Derived Imidazole for Improved Flame Retardancy and Smoke Suppression of Epoxy Resin. *ACS Appl. Polym. Mater.* **2020**, *2* (8), 3566−3575.
(56) Berne, D.; Ladmiral, V.; Leclerc, E.; Caillol, S. Thia-Michael Reaction: The Route to Promising Covalent Adaptable Networks. *Polymers* **2022**, *14* (20), 4457.
(57) Yao, B.; Mei, J.; Li, J.; Wang, J.; Wu, H.; Sun, J. Z.; Qin, A.; Tang, B. Z. Catalyst-Free Thiol−Yne Click Polymerization: A Powerful and Facile Tool for Preparation of Functional Poly(Vinylene Sulfide)S. *Macromolecules* **2014**, *47* (4), 1325−1333.
(58) Oishi, Y.; Kim, J. J.; Nakamura, M.; Hirahara, H.; Mori, K. Synthesis of Polysulfides Containing S-Triazine Rings from 6-Substituted Amino-1,3,5-Triazine-2,4-Dithiols and 1,10-Dibromodecane. *Macromol. Rapid Commun.* **1999**, *20* (5), 294−298.
(59) Daglar, O.; Gunay, U. S.; Hizal, G.; Tunca, U.; Durmaz, H. Extremely Rapid Polythioether Synthesis in the Presence of Tbd. *Macromolecules* **2019**, *52* (9), 3558−3572.
(60) Xue, F.; Si, Y.; Wang, M.; Liu, M.; Guo, L. Toward Efficient Photocatalytic Pure Water Splitting for Simultaneous H2 and H2o2 Production. *Nano Energy* **2019**, *62*, 823−831.
(61) Lu, S.; Shen, B.; Chen, X. Construction of Charring-Functional Polyheptanazine Towards Improvements in Flame Retardants of Polyurethane. *Molecules* **2021**, *26* (2), 340.
(62) Zhu, M.; Yu, S.; Ge, R.; Feng, L.; Yu, Y.; Li, Y.; Li, W. Cobalt Oxide Supported on Phosphorus-Doped G-C3n4 as an Efficient Electrocatalyst for Oxygen Evolution Reaction. *ACS Appl. Energy Mater.* **2019**, *2* (7), 4718−4729.
(63) Kumar, A.; Solanki, A.; Nguyen, W. H. C. H.; Henni, A. Determination and Prediction of Dissociation Constants and Related Thermodynamic Properties for 2-(Butylamino)Ethanol, M-Xylylenediamine, 3-Picolylamine, Isopentylamine, and 4-(Aminoethyl)-Piperidine. *J. Chem. Eng. Data* **2020**, *65* (11), 5437−5442.
(64) Bünger, H. Ullmann's Encyclopedia of Industrial Chemistry, Vol. A 12 Formamides to Hexamethylenediamine. Vch, Weinheim−Basel−Cam−Bridge−New York 1989. Xv, 632 S., 253 Abb., 156 Tab., Geb., Dm 520,−. *Chem. Ing. Technol.* **1990**, *62* (5), 434−434.
(65) Li, Z.; Wei, P.; Yang, Y.; Yan, Y.; Shi, D. Synthesis of a Hyperbranched Poly(Phosphamide Ester) Oligomer and Its High-Effective Flame Retardancy and Accelerated Nucleation Effect in Polylactide Composites. *Polym. Degrad. Stab.* **2014**, *110*, 104−112.
(66) Perret, B.; Schartel, B.; Stöß, K.; Ciesielski, M.; Diederichs, J.; Döring, M.; Krämer, J.; Altstädt, V. A New Halogen-Free Flame Retardant Based on 9,10-Dihydro-9-Oxa-10-Phosphaphenanthrene-10-Oxide for Epoxy Resins and Their Carbon Fiber Composites for the Automotive and Aviation Industries. *Macromol. Mater. Eng.* **2011**, *296* (1), 14−30.
(67) Rayaroth, M. P.; Escobedo, E.; Chang, Y.-S. *Chapter Nine—Degradation Studies of Halogenated Flame Retardants*. In Comprehensive Analytical Chemistry, Oh, J.-E., Ed.; Vol. *88*; Elsevier, 2020; pp 303−339.
(68) Ortega-Olvera, J. M.; Mejía-García, A.; Islas-Flores, H.; Hernández-Navarro, M. D.; Gómez-Oliván, L. M. *Chapter Three—Ecotoxicity of Emerging Halogenated Flame Retardants*. In Comprehensive Analytical Chemistry, Oh, J.-E., Ed.; Vol. *88*; Elsevier, 2020; pp 71−105.

https://doi.org/10.1021/acs.macromol.4c01288
Macromolecules 2024, 57, 9396−9407